



Trade Science Inc.

Materials Science

An Indian Journal

Full Paper

MSAII, 6(1), 2010 [21-30]

The role of decylamine template of the size control on mesoporous materials

Mohamed A.Betiha^{1,*}, Mohamed F.Menoufy¹, Maged S.Ghattas¹, Hussien Abd El-aziz¹,
Essam M.Ezzo²

¹Refining Department, Egyptian Petroleum Research Institute, Cairo 11727, Nasr City, P.O. Box 9540, (EGYPT)

²Chemistry Department, Faculty of Women for Art, Science and Education, Ain Shams University, (EGYPT)

E-mail : Mohamed_betiha1@yahoo.com

Received: 2nd January, 2010 ; Accepted: 12th January, 2010

ABSTRACT

The low-temperature formation of liquid-crystal-like arrays made up of molecular complexes formed between molecular inorganic species (TEOS) and neutral organic molecule (Decylamine) is a convenient approach for the synthesis of mesostructure materials. Mesoporous silicates structure with controlled pore sizes (2– 4 nm) were successfully synthesized from tetraethoxysilane (TEOS) using mixture of decylamine (DA) as template and different organic solvent (ethanol, 1,4-dioxan or benzene). The auxiliary mixture of DA and TEOS act as a swelling agent for DA and functionalized silica. By adjusting the initial molar ratio of DA/TEOS from (0.252 - 0.166), pore and the particle sizes of the final disordered hexagonal mesoporous silicas could be precisely tuned in the ranges of 2-4 nm and 320 -540 nm respectively. Solvent structure direction can be effectively used to control the surface area and the pore size by varying their polarity. Results show that the hydrogen bonds between the condensed silica and NH₂ group using different solvents, disordered hexagonal structure of mesostructured silica was obtained at different concentration of NH₂. The HMS samples were characterized using thin film X-ray, N₂ adsorption-desorption, scanning electron microscopy (SEM), and transmission electron microscopy (TEM). © 2010 Trade Science Inc. - INDIA

KEYWORDS

HMS;
Mesoporous molecular
sieve synthesis;
Swelling agent;
Nanosized microemulsion.

INTRODUCTION

Designing a heterogeneous catalyst involves both the proper control of the surface chemistry and a rigorous control of the surface geometry at the micro-, meso- and macroscales. This is because high surface areas or high active phase dispersions as well as fast mass transfer of the reactants and products to and from the catalytic sites are required from any active catalyst.

It is, therefore, clear that the new materials designated as mesoporous molecular sieves (MMSs) have introduced a new degree of freedom in the conception of catalysts. Indeed, MMSs are very high surface area materials (ca \approx 1200 m² g⁻¹ for mesostructured silica) having mono-dispersed pore diameters in the range 2– 50 nm and a stereoregular arrangement of these channels which mimics the liquid crystals formed by the surfactants used in their preparation^[1-3]

Full Paper

The first one is the so-called M41S family of silica and aluminosilicates introduced by the Mobil group^[4-6] which includes hexagonal MCM-41, cubic MCM-48 and lamellar MCM-50 phases. The preparation of M41S follows an ionic assembly mechanism schematically represented as S⁺I. This mechanism was extended by Stucky and co-workers to a whole series of other electrostatic assembly mechanisms, including a reversed S⁻I⁺ and counter-ion mediated S⁺XI⁺ and S⁻M⁺I pathways^[7,8].

The second one was introduced by the group of Pinnavaia who produced MMSs using two neutral routes based on hydrogen bonding and self assembly of non-ionic primary amines and neutral oligomeric silica precursors S⁰I⁰^[9-11]. The hexagonal mesoporous silica (HMS) produced by this technique are less ordered, showing a wormhole like pore structure, than MMS's produced with ionic surfactants. They have, however, a monodispersed pore diameter, thicker pore walls, a higher degree of condensation, and therefore, a higher thermal stability.

The pore diameters in the range of 2–10 nm are possible, depending on the precursors, templates, and reaction conditions. In addition, varying the processing parameters allows for the production of materials with different appearances, such as films, powders, or monoliths. Various applications for porous materials are under consideration, for example, as catalyst supports and membranes,^[12,13] and many of these require a deliberate control of the pore size and orientation. The textural mesoporosity plays a key role in the catalytic reactivity enhancement and its presence depends on the synthesis conditions especially when a water-rich solvent is used^[14].

The synthesis of mesoporous silicate materials in aqueous conditions using primary amine as templates, some organic hydrocarbon molecules such as mesitylene (TMB)^[15] and, hexane, nonane, etc.^[16,17] can be used as pore size swelling agents. The hydrocarbon molecules can interact with the hydrophobic segment as a result, the lattice is enlarged or the phase transition occurs. Burleigh et al.^[18] used 1,2-bis(trimethoxysilyl)ethane and Pluronic P123 (EO₂₀PO₇₀EO₂₀), and the reaction mixtures were treated with various amounts of the swelling agent TMB. The pore diameters increased from 6 to 20 nm with

increasing concentrations of TMB, while the pore structure changed from wormlike to a hexagonal arrangement of spherical pores.

Liang and Anwender^[19] synthesized ethane-bridged periodic mesoporous organosilicas (PMOs) form in the presence of a binary surfactant mixture under basic conditions whereby the mixture consisted of the gemini surfactant and CTAB. The products had only a relatively low degree of order, but by adding typical swelling agents such as TMB or 1,3,5-triisopropylbenzene to the binary surfactant mixture. Those authors' data indicate the increase in pore diameter considerably. The materials prepared with swelling agents exhibited pore diameters up to 11 nm.

In the present work, texture performance is studied in which the synthesis of HMS morphology have particularly promise, because of their relatively large specific surface area and pore volume, suitable pore size, tight pore-size distribution and ordered structure. For this purpose, mono-disperse, micrometer-sized spherical particles are essential. There are few reports in the literature that describe the synthesis of spherical mesoporous particles using organic solvents for controlling pore diameter. The structure parameters of prepared materials were evaluated using X-ray diffraction (XRD), N₂ adsorption–desorption, scanning electron microscope (SEM) and transition electron microscope (TEM).

EXPERIMENTAL

Chemicals

All materials were used without further purification; Decylamine (DA) and tetraethylorthosilicate (TEOS) were purchased from Sigma Aldrich. Ethanol, dioxan and benzene were obtained from fluka.

Synthesis of mesoporous silica

Hexagonal mesoporous silica (HMS) was synthesized by the neutral S⁰I⁰ templating route, proposed by Tanev and Pinnavaia^[14,15,20], which is based on hydrogen bonding and self-assembly between neutral primary amine surfactants (S⁰), decylamine, and a neutral inorganic precursor (I⁰), tetraethylorthosilicate. The reaction is modified by using different organic solvents; ethanol or dioxan or benzene as swelling agent. 10 g (0.048

mol) of TEOS was added to a homogeneously stirred solution of x g of $\text{CH}_3(\text{CH}_2)_9\text{NH}_2$, 10 gm of organic solvent and 90 g of distilled water. HMS-I_a was prepared using the reagent quantities given in TABLE 1, according to the following steps:

Step 1, 1.9 g of DA was stirred in 90 mL of water and 10 mL of EtOH for 30 min until an opalescent mixture was obtained.

Step 2, TEOS was added to that from Step 1 very slowly for 1 h.

Step 3, the mixture from Step 2 was kept at rest for 20 h at room temperature to obtain product. The as-synthesized HMS-I_a was separated by filtration, washed with ethanol several time, dried at room temperature and finally calcined at 550 °C for 6 h in air, at a heating rate of 1 °C min⁻¹. The other samples HMS-I_{b,c} were prepared by the same procedure with different ratio (0.2 and 0.16 mol %) of the same solvent as shown in TABLE 1. HMS-II and HMS-III were obtained with the same producer using dioxan and benzene respectively.

TABLE 1 : Preparation of hexagonal mesoporous silica (HMS) using decylamine

Code ^(a)	TEOS g	DA g	H ₂ O g	Swelling agent ^(b)
HMS-I _a	10 g (0.048 mol)	1.257 g (0.008 mol)	90 g	10 gm
HMS-I _b	10 g (0.048 mol)	1.573 g (0.01 mol)	90 g	10 gm
HMS-I _c	10 g (0.048 mol)	1.9 g (0.012 mol)	90 g	10 gm
HMS-II _a	10 g (0.048 mol)	1.257 g (0.008 mol)	90 g	10 gm
HMS-II _b	10 g (0.048 mol)	1.573 g (0.01 mol)	90 g	10 gm
HMS-II _c	10 g (0.048 mol)	1.9 g (0.012 mol)	90 g	10 gm
HMS-III _a	10 g (0.048 mol)	1.257 g (0.008 mol)	90 g	10 gm
HMS-III _b	10 g (0.048 mol)	1.573 g (0.01 mol)	90 g	10 gm
HMS-III _c	10 g (0.048 mol)	1.9 g (0.012 mol)	90 g	10 gm

^(a)is represent the molar ratio of DA to TEOS. ^(b)is represent type of organic solvent ethanol or dioxan or benzene: HMS-I, HMS-II, HMS-III were synthesized using ethanol, dioxan and benzene respectively.

Characterization

X-ray diffraction patterns of the sample were recorded using a Pan Analytical Model X' Pert Pro, which

was equipped with CuK α radiation ($\lambda = 0.1542$ nm), Ni-filter and general area detector. The diffractograms were recorded in the 2θ range of $0.5 - 70^\circ$ with step size of 0.02° and a step time of 0.605.

Nitrogen adsorption/desorption isotherms of the synthesized HMSs samples were obtained using NOVA 3200 (USA), at -196°C (77 K) after degassing at 300°C and 10^{-5} mm Hg for 4 h. The BET surface area (S_{BET}) of the investigated samples was calculated from adsorption isotherm data using the BET method. Pore size distribution (PSD) curves were calculated from the adsorption branch of the isotherms using the Barrett-Joyner-Halenda (BJH) method. The adsorption branch was favored over desorption branch in order to avoid the tensile strength effect (TSE) artifact which very often complicates the PSD determination in mesoporous systems. The total mesopore volume were calculated by the BJH method from desorption branch at $P/P_0 \sim 0.98$.

Thermal analysis (DSC-TGA) was carried out for the HMSs samples using simultaneous DSC-TGA SDTQ600 (TA-USA) in dry N₂ atmosphere with heating rate $10^\circ\text{C min}^{-1}$ in the range up to 600°C .

SEM measurement was performed on electron microscope JEOL JEM 5300 under vacuum condition at bar pressure. Scanning Electron Microscopy was carried out in order to determine the morphology of the sample and the crystal size. Before the measurement, samples were mounted over sample holder (stubs) using double sided tape. The sample was further coated with gold using Sputter Coating System at 10 mbar with current flow 15 mA.

Transmission electron microscopy (TEM) studies were carried out using a JEOL JEM microscope operating at 120 kV. The calcined catalysts were crushed and dispersed ultrasonically in water at room temperature and then spread onto a perforated carbon-copper microgrid.

RESULTS AND DISCUSSION

Effect of preparation condition

Hydrogen-bonding interaction mechanisms, namely, S^oI^o where S^o are neutral amines, and I^o are hydrated silicate oligomers from TEOS, was proposed by Pinnavaia and co-workers for preparing mesoporous

Full Paper

silicates under neutral conditions^[21,22]. Long-chain alkyl amines, such as primary alkylamines have hydrophobic hydrocarbon chains and hydrophilic amine groups, similar to surfactants^[21]. However, some swelling agents were to be added in the synthesis batch for mesoporous silicas due to the insolubility of these amines^[21,23].

Silicate oligomers are negatively charged in basic solution. There is a distinct two functionalization strategies considered for the preparation of hybrid inorganic-organic frameworks (HMS). The first incorporation approach, denoted as the *template alkaline catalyzed pathway*, involves the hydrolysis of TEOS and physical interaction between decylamine and $\text{Si}(\text{OH})_4$ depending on amine ratio. The morphology of the structure-directing micelle is expected to remain unperturbed by the inclusion of the relatively large functional moieties in which the concentration and size of the organic group is the increased because of the high swelling of the templating amine leading to more interparticle mesoporosity. The distribution of charge density in matrix is highly varied due to the very high competition between hydrolysis, self-condensation and co-condensation in alkaline medium.

The second incorporation approach, denoted as the *direct addition pathway*, entails the incorporation of further inorganic moieties over the first nucleus formed that preventing penetration into lattice of structure formed due to low pH of medium. This latter strategy is expected to favor the incorporation of inorganic moieties whose dimensions are significantly smaller than those of the amine functionalized.

XRD analysis

Figure 1-3 provide the X-ray powder diffraction patterns for the prepared samples HMS-I-III derivatives assembled from DA as the structure director and organic solvent as swelling agents. Figure 1-2 provide Structures formed using ethanol (HMS-I) and dioxan (HMS-II) showed qualitatively equivalent diffraction features. All patterns contain a strong, relatively broad reflection at $2.0\text{--}3.0^\circ 2\theta$ and a very weak broad shoulder in the region near $4.0^\circ 2\theta$ due to small scattering domain sizes. These patterns are typical of HMS worm-hole structures assembled from long alkyl chain neutral amines as surfactants, the correlation peak indicating the average pore-pore separation in the disordered wormhole framework.

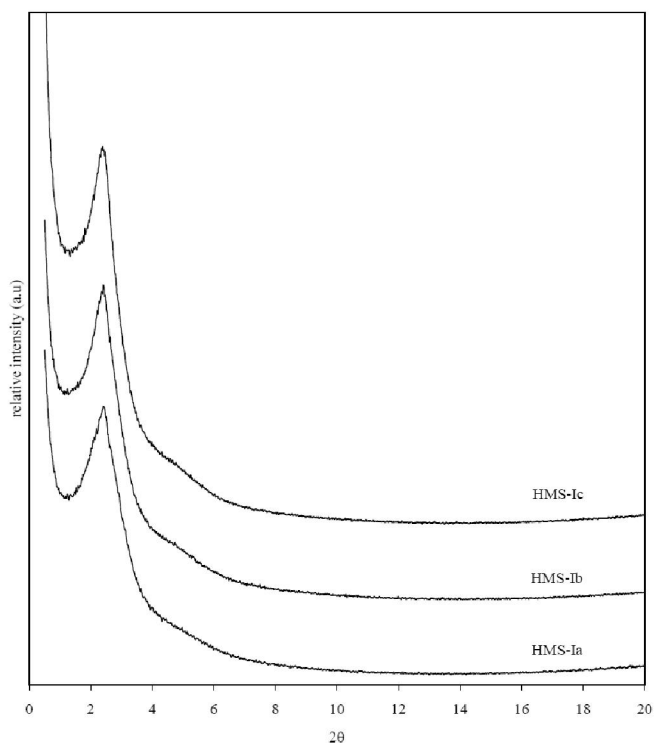


Figure 1 : XRD patterns of calcined silica materials obtained following the synthesis procedure for HMS-I using

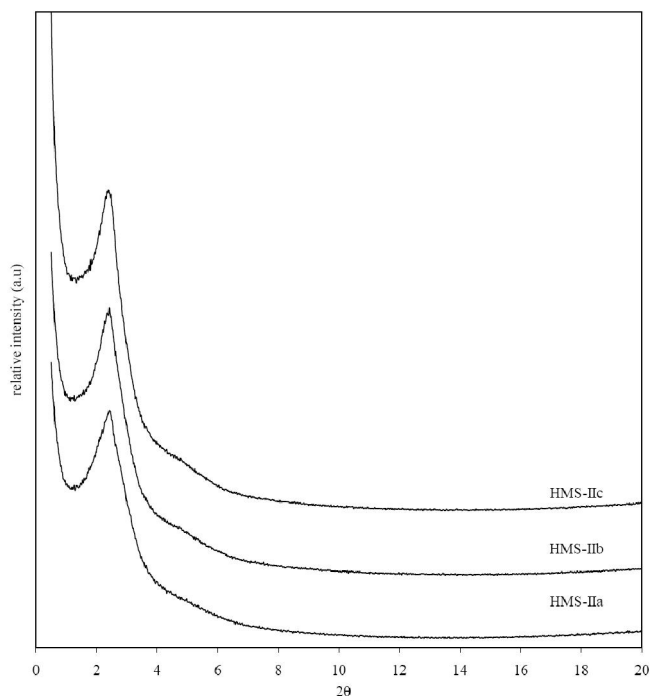


Figure 2 : XRD patterns of calcined silica materials obtained following the synthesis procedure for HMS-II using DA.

The qualitative form of the patterns is affected by the amine concentration or by the presence of ethanol or dioxan. However, the positions of the intense reflection and the weak broad shoulder are depending on

amine concentration and the polarity of the reaction medium. Also; it is clear that with increasing amine concentration the intensity increases indicating more ordered structure.

Figure 3 shows XRD of HMS-III, the main intense peak of HMS shifted towards higher d -spacing ($2\theta \approx 1.35^\circ$) than HMS-I & HMS-II ($2\theta \approx 2.4^\circ$). In addition, the main peak became less broad and more intense, suggesting a crystalline nature of the material. Moreover, the reflections peak of different amine concentrations are slightly equal indicating benzene remained trapped on different concentration of DA species and the difference of polarity between water and benzene fixed the micelles radius. As the amine concentration ratio increases, from 0.16 to 0.25, the aggregation increased that might affect the wall thickness characteristics. Swelling agent, benzene, increase the unit cell parameter value than ethanol and dioxan. The reason of increasing the unit cell parameter value of HMS-III likely is difference in chemistry between starting gels, influencing the micellar size and course of crystal growth. With an decrease of NH_2/Si ratio in all cases, a gradual increase of long-range order is observed by a increase of intensity of the diffraction peaks, which is probably

due to increasing the association number and more tight aggregation of amine micelles lead to a higher hindrance of the hydrophilic amine moiety to be penetrated than in case of ethanol and dioxan.

The broadness of different peaks at different DA/TEOS ratio can be related to the variation of the pH value of media during the synthesis time. pH is distinctly raised at the beginning, caused by the hydrolysis of silicates and then slightly reduced due to the crosslinkage of silica species. Owing to the weak alkalinity of DA, disordered mesoporous silica materials are sometimes obtained with it. With increasing pH value of auxiliary mixture, the polymerization rate of $\text{Si}(\text{OH})_4$ increase due to the high condensation rate and pronounced gel effect. The gel effect is mostly important because it causes random polymerization and leads to an increase in the overall polymerization rate and crosslinking.

Nitrogen adsorption-desorption isotherms

The surface properties of the mesoporous HMS derivatives (BET surface area, pore volume, and pore diameters) were determined from the N_2 adsorption isotherms are given in TABLE 2.

TABLE 2

Support	$2\theta(^{\circ})$	d_{100} (nm)	α_0 (nm)?	S_{BET} (m^2/g)	V_{P} (cm^3/g)	D (nm)	L (nm)
HMS-I _a	2.45	3.6	12.471	921.36	0.5344	2.068	10.403
HMS-I _b	2.43	3.63	12.575	434.63	0.7988	2.274	10.301
HMS-I _c	2.39	3.69	12.783	1195.72	1.0600	2.632	10.151
HMS-II _a	2.45	3.6	12.471	987.68	0.5940	2.102	10.369
HMS-II _b	2.43	3.63	12.575	1167.96	0.7597	2.202	10.373
HMS-II _c	2.40	3.68	12.748	1191.33	0.9202	2.450	10.298
HMS-III _a	1.45	6.09	21.096	444.79	0.4720	3.830	17.266
HMS-III _b	1.35	6.54	22.655	598.12	0.6572	3.890	18.765
HMS-III _c	1.23	7.17	24.837	648.24	0.8593	3.960	20.877

Surface area calculated from BET equation.

Pore volume calculated from the adsorption branch of the isotherm at $P/P_0 \approx 1$.

Pore diameter (D) calculated from the adsorption branch of the isotherm according to BJH method.

L, pore wall thickness; $L = \alpha_0 - D$, α_0 , interplanar spacing corresponding to hexagonal structure in [100] direction.

α_0 is the unit cell parameter calculated from the XRD distance by $\alpha_0 = 2d_{100} / \sqrt{3}$.

The nitrogen adsorption isotherms of the HMS are shown in Figure 4-6. All the isotherms of HMS samples showed type IV with type H1 hysteresis loops typical of mesoporous materials with 1-D cylindrical channels, giving very strong evidence that all HMS materials have

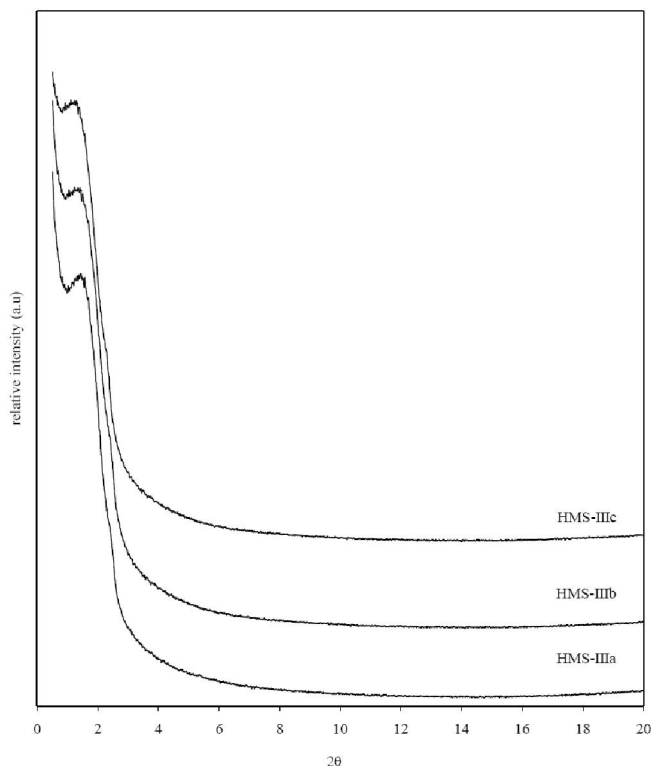


Figure 3 : XRD patterns of calcined silica materials obtained following the synthesis procedure for HNS-III using DA.

Full Paper

mesoporous and cylindrical pores structures^[22-25].

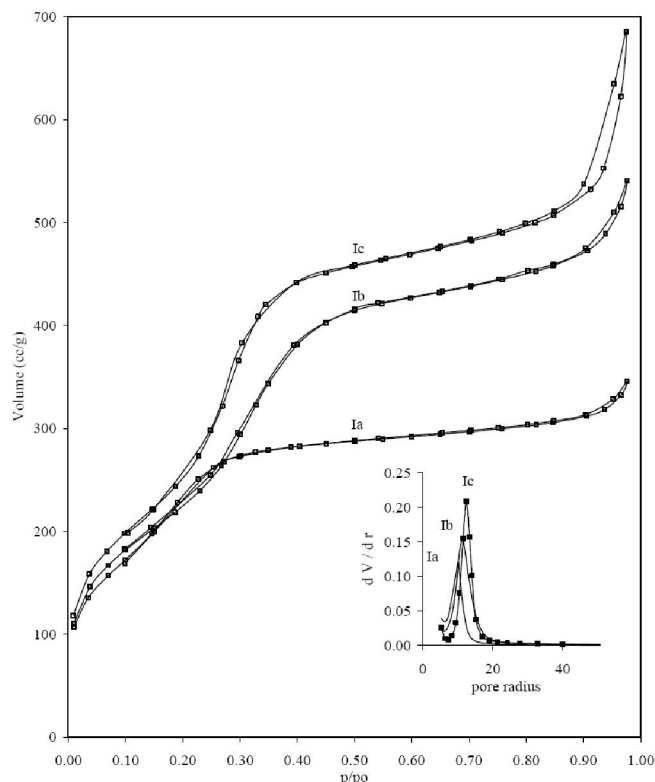


Figure 4 : N₂ gas adsorption–desorption isotherm and pore size distribution plots of HMS-I

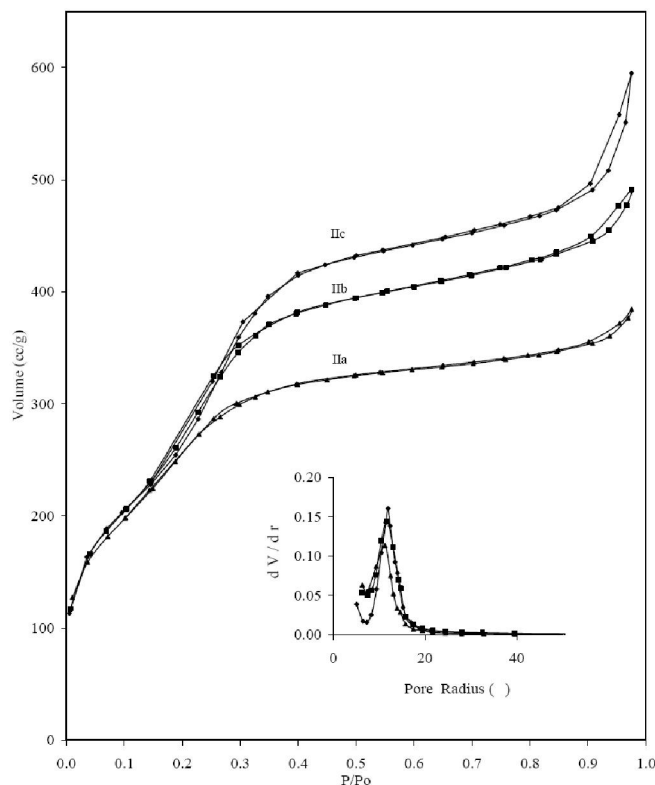


Figure 5 : N₂ gas adsorption–desorption isotherm and pore size distribution plots of HMS-II

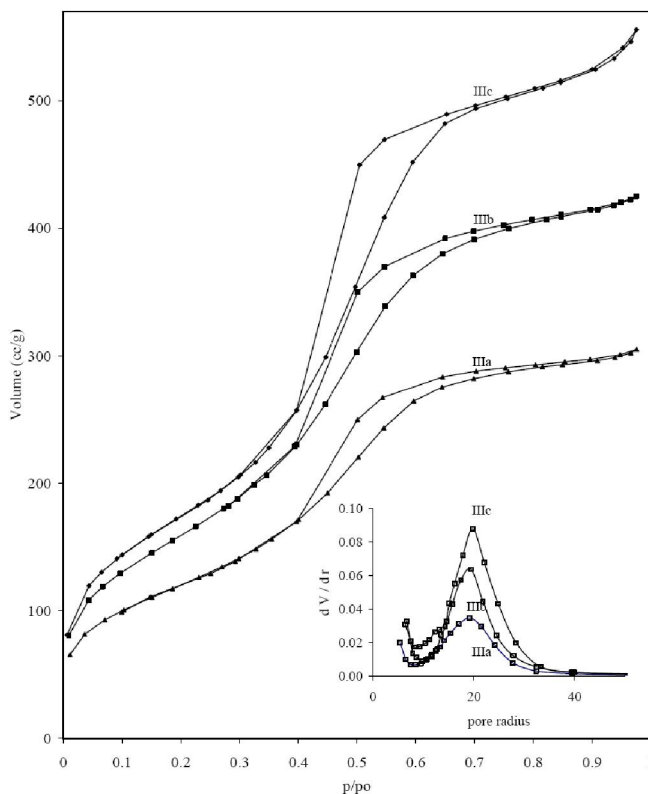


Figure 6 : N₂ gas adsorption–desorption isotherm and pore size distribution plots of HMS-III

Figure 4&5 showed typical isotherm of HMS-I and HMS-II. With increasing DA/TEOS ratio the volume of nitrogen absorbed increased due to the high porosity. At a relative low nitrogen pressure of approximately 0.15 a sudden step increase of the amount of adsorbed nitrogen is observed. This step increase is caused by capillary condensation of nitrogen inside the mesopores and directly proportional to amine concentration, i.e. the mesopores of HMS become suddenly filled by liquid nitrogen. Because filling of the mesopores takes place over a relatively small range of relative pressures (i.e. $p/p_0 \approx 0.15-0.40$), the pores associated with this process must be nearly equal in size.

The first hysteresis loop, which starts at a relative pressure of 0.15–0.40, indicates the presence of framework mesoporosity, whereas the second hysteresis loop, which starts at a relative pressure of about 0.80–0.95 in high concentrated amine, is due to textural interparticle mesoporosity or macroporosity. These patterns are typical of HMS wormhole structures assembled from long alkyl chain neutral amines as surfactants^[21].

In addition, the adsorption of HMS-I & HMS-II were near flat at different amine concentrations and

show two adsorption loops extended over a large range of relative pressures (i.e. $\approx 0.4-0.9$), indicating the presence of both meso- and macroporosity. The flatness indicates that all pores have equal size. However the flatness was indirectly proportional with increasing DA/TEOS ratio which indicates the most equal porosity attained from low ratio of DA/TEOS. The desorption curve almost completely coincides with the adsorption isotherm in this pressure range, giving a very narrow hysteresis loop (i.e. the difference between the adsorption and desorption curves). Moreover, the shapes of the curves and the hysteresis loop are very characteristic for cylindrical mesopores.

Figure 6 showed the N_2 sorption isotherms and pore-size distribution plots of HMS-III materials with varied DA/TEOS ratio. The adsorption branched of each isotherm shows a sharp inflection in the relative pressure range of about 0.4-0.65. This is a characteristic of capillary condensation with uniform mesopores. The position of the P/P_0 inflection points is related to the pore size in the mesopores range, and the sharpness of these steps indicates the uniformity of the pore size. Besides, the HMS-III samples present a single modal pore size distribution centered around 3.8 nm.

As can be seen from TABLE 2, pore sizes of HMS-III materials has no big change when increasing the DA/TEOS ratio with approximately high change in unit cell parameter. These results imply that the benzene oriented at same location of micelles structures or amine micelle centered at same radius. The difference in surface area was related to nature of auxiliary mixture. The viscosity increment and gelation of liquid crystal liquid mixture have been attributed to the expansion of surfactant tails and the structure formation among the micelle due to strong interactions at the tail-to-tail and face-to-face contacts. The elongation of micelles is a consequence of the reduction of polarity and water content within the micelles due to the adsorption and polymerization of silicate species. Moreover, it was found that the extent of the amine chains located within the silica mesopores depended on both the solvent type and the Si/NH_2 molar ratio.

Three different solvent are used to prepare hexagonal mesoporous silica (HMS). Two of them are protic (ethanol and dioxan) while the third is aprotic (benzene). Ethanol is one of the products formed dur-

ing the sol-gel synthesis, and thus addition of ethanol reduces the reaction rate, which in turn decreases the local surface curvature energy and leads to the formation of curved morphologies^[26]. Also, ethanol will solvate the head of primary amine, increases head group size and prevent penetration of condensed silica. Dioxan has the ability to solve both head and tail of alkylamines, increasing the distribution of micelles in dioxan/water system i.e. broad surface. Benzene solvate the tail of alkylamine, more increase the hydrophobic tail, leading to an increase in the radius of micelle as the pH decreases. Benzene has low polarity that will decrease the polarity of mixture so both hydrophilic ($\equiv Si-OH$) segments can not interact with these solvents and cause more repulsion with condensed silica.

Also; increasingly polar of auxiliary mixture (in case of dioxin and ethanol) partition the surfactant toward homogeneous solution while low polarity solvent (benzene) partition the surfactant between homogeneous solution and emulsion forms.

The homogeneous solution suggested that the silica primary particles are not nucleated but they participated at/between surface colloidal particles of the free surfactant in emulsion form. As silica primary particles undergo further intergrowth and diminish the emulsion, prevent the segregated surfactant forms within aggregates and high textural porosity was obtained. So, the broadness of pore size distribution (PSD) indicated in (Figure 4-6) may be results from two functions; (1) the curvature between silica aggregates, (2) the pores form surfactant micelle. While in case of heterogamous mixtures of HMS-III derivatives, in which the textural mesoporosity can be as high as indicated from sharp steepness at $p/p_0 = 0.4$ (Figure 6) than HMS-I & HMS-II. The strong correlation between high textural mesoporosity and surfactant heterogeneity suggests that primary HMS particles are nucleated from the heterogeneous solution phase including surfactant aggregates without deplete of the surfactant mixture. Most of silica particle precipitated of surfactant/silica nucleus and high mesoporosity was obtained.

Also amine concentration plays another interesting role for controlling both pore sizes and surface area. In the alkaline medium the silicate is negatively charged. So in the alkaline route, amine and silicates were organized by weak repulsion between NH_2 and negative silica,

Full Paper

leading to more expansion in pore diameter. Because of the higher polymerization rate, the $\equiv\text{Si}(\text{OH})$ quickly become jelly, with the result that it is more difficult for $\equiv\text{Si}(\text{OH})$ to insert into micelle. As amine concentration decreases there is a competition between polymerization inside micelle and outside micelle due to different nature of auxiliary mixture during polymerization time.

SEM

The particle size distributions of different DA/TEOS molar ratio of the synthesized samples were summarized in Figure 7 & TABLE 3. It can be found that the particle sizes are large when ethanol is used, and turns smaller in case of dioxan. The small particle size was in order HMS-IIc, HMS-IIIc and HMS-Ic respectively. The probable reasons may be described as follows: (1) nature of solvent increase the template micelles concentration that decreases the surface tension till micelles are formed at the critical micelle concentration (CMC), and the low surface tension favors to generate more nucleuses which lead to particle sizes reduction. Dioxan decreases the polarity of water that increasing supersaturation degree of gel. Supersaturation degree is the

TABLE 3 : Particle size distribution of HMS synthesized at different solvent

Support	Range of particle size/nm
HMS-Ic	100 ~ 630
HMS-IIc	320 ~ 390
HMS-IIIc	340 ~ 740

main driving force of crystal nucleus generation. (2) Renzo^[27] considered that the rate of nucleation and the growth of crystals will enhance with the increasing supersaturation degree. The grain size depends on the ratio of nucleation rate to crystals growth rate. The increase of supersaturation degree helps to raise this ratio and results in reducing particle size. Also, reduction in particle size may be due to the lower interfacial tension which helps to dissolve template reagent in solution. So we can expect that the quantity of dioxan can dissolved DA completely and smaller particle size can be presented.

The TEM photos of the HMS-Ic, HMS-IIc and HMS-IIIc mesoporous materials showed the changes in the size and arrangement of the mesopores according to swelling type. As shown in Figure 8, worm-like

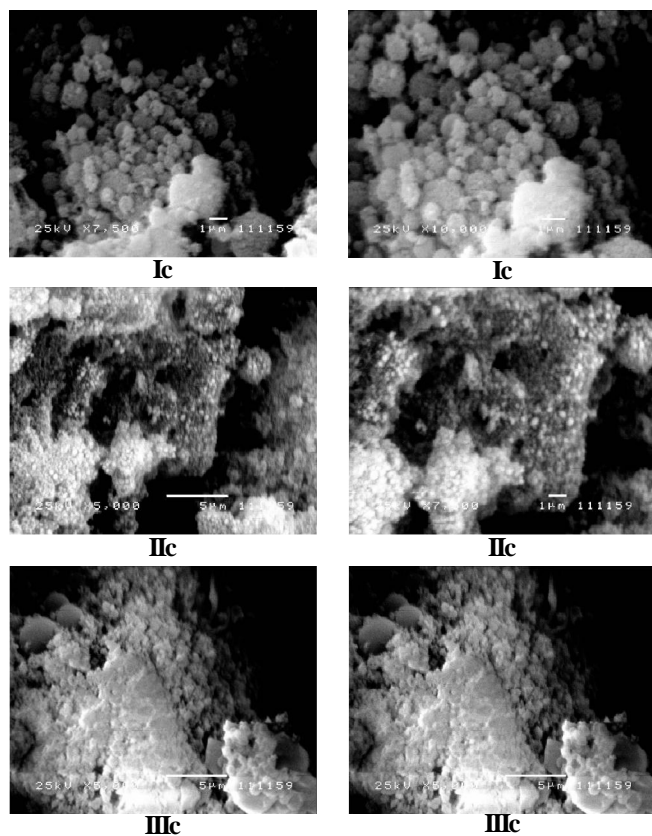


Figure 7 : SEM of HMS-IIIa, HMS-IIIb and HMS-IIIc

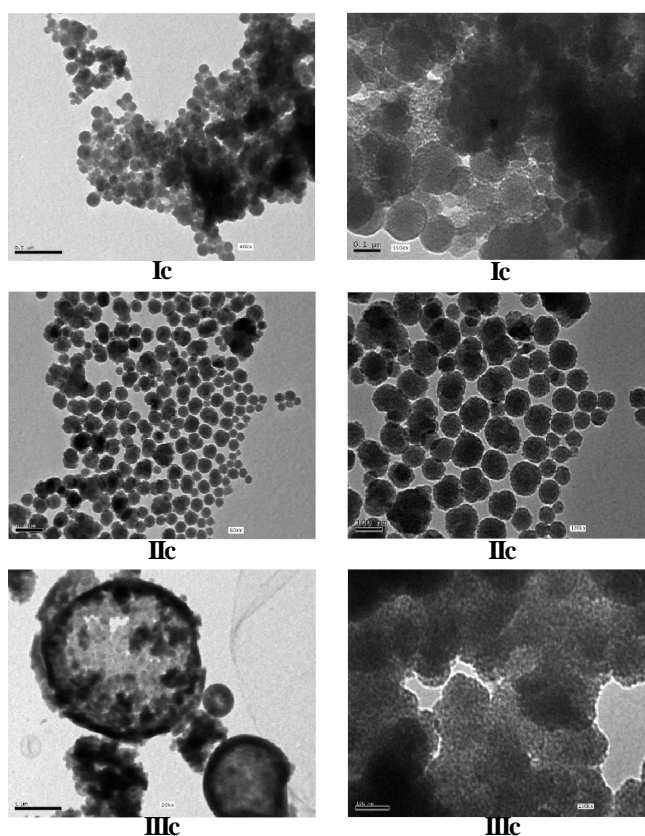


Figure 8 : SEM of HMS-IIIa, HMS-IIIb and HMS-IIIc

disordered mesopores with a small diameter. The arrangement of the mesopores was not altered on HMS-IIIc prepared using the hydrophobic solvent, but the increase in the diameter of the mesopores was certain.

There was no regularity in the arrangement of the mesopores of all prepared samples. However, the mesoporous material prepared using dioxan, showed nicely ordered mesopores. No diffraction spot was observed on the HMS-I-IIIc mesoporous materials due to their worm-like disordered mesopores.

Thermogravimetric analysis (TGA)

TGA is a useful technique to gain information about the interaction of template with Si atoms present in the mesoporous materials^[28]. The thermogram of uncalcined HMS-Ib is shown in Figure 9. It can be seen that there is a rapid weight loss in 50–280 °C region. The thermal behavior of washed and uncalcined HMS-Ib sample is represented in Figure 9. Positive peaks indicate exothermic processes whereas negative peaks represent endothermic processes. Two endothermic peaks were detected below 250 °C. The first peak occurred at 100 °C and was likely due to evaporation of moisture or solvent adsorbed to the

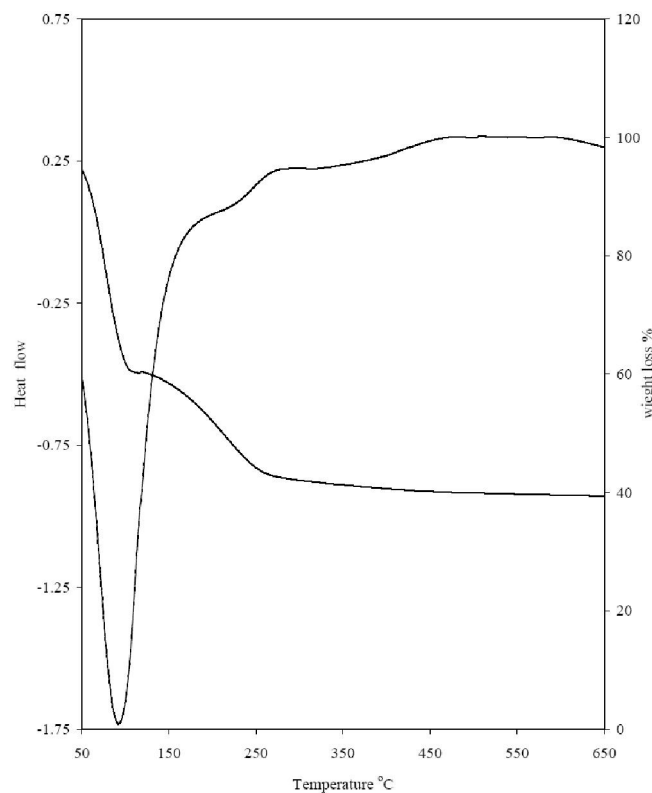


Figure 9 : DSC (left) and TGA (right) curves of uncalcined HMS-Ib materials as a function of DA/TEOS ratio.

surface of particles. The second endothermic peak occurred at 230 °C was assigned to interaction of remained DA with silanol groups, which accompanied by weight loss in TG curve. There is no specific peak to indicate the phase transformation.

Figure 10 showed the TGA analysis for some calcined sample. All sample showed excellent thermal stability and the weight loss was observed from 370 to 650 °C due to the dehydroxylation of the surface. It is clear that the dehydroxylation decrease with increasing DA/TEOS ratio. This behavior can be explained by the fact that the more silanol groups can be consumed during the reaction at high DA concentration.

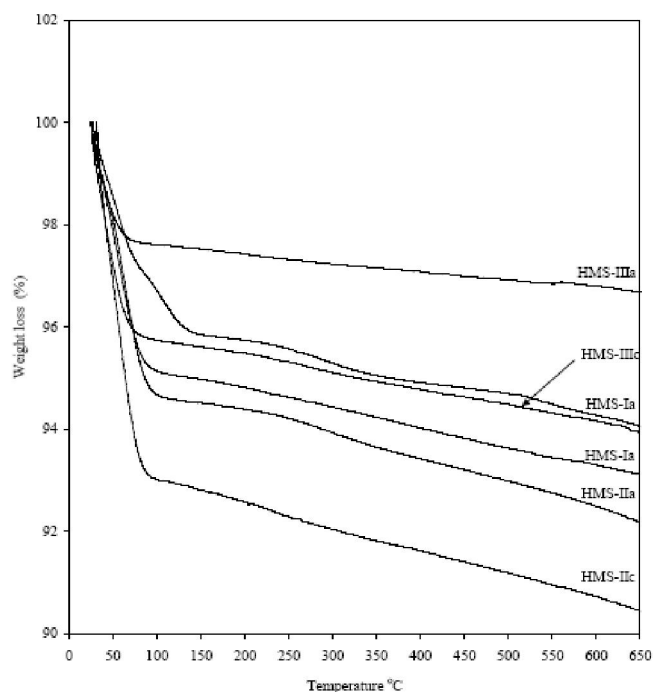


Figure 10 : TGA of calcined HMS-I, HMS-II and HMS-III

CONCLUSION

HMS molecular sieve has been synthesized via hydrogen bonding self assembly in microemulsion. The results indicate that the HMS sample with high surface area, controlled pore size and particle size can be prepared under different condition. An increase in amine concentration gives high surface area and high porosity. Particle size around 200–300 nm can be obtained under using protic solve as swelling agent.

The textural properties of HMS molecular sieves with wormhole framework structures are determined by the physical state of the neutral amine surfactant used

Full Paper

to direct the S^oP assembly process. Homogeneous solutions of the structure directing surfactant in water/ethanol and water/dioxin cosolvents completely dissolve the surfactant and allow for the formation of HMS derivatives with high textural mesoporosity. The uniform nucleation and growth of HMS derivatives from these homogeneous surfactant solutions results in monolithic particles with smooth surfaces, as judged by SEM. The textural properties of HMS derivatives are similar to those of hexagonal MCM-41 mesostructures assembled through electrostatic assembly pathways. Textural porosity is dependent on the size, connectivity, and surface texture of the fundamental particles, but it is independent of the framework structure of the particles.

REFERENCES

- [1] C.T.Kresge, M.E.Leonowicz, W.J.Roth, J.C.Vartuli, J.S.Beck; *Nature*, **359**, 710-712 (1992).
- [2] T.Yanagisawa, T.Shimizu, K.Kuroda, C.Kato; *Bull.Chem.Soc.Jpn.*, **63**, 988-992 (1990).
- [3] A.Monnier, F.Schueth, Q.Huo, D.Kumar, D.Margolese, R.S.Maxwell, G.D.Stucky, M.Krishnamurty, P.M.Petroff, A.Firouzi, M.Janicke, B.F.Chmelka; *Science*, **261**, 1299-1303 (1993).
- [4] C.T.Kresge, M.E.Leonowicz, W.J.Roth, J.C.Vartuli; US Patent 5,098,684, (1992).
- [5] J.C.Vartuli, C.T.Kresge, M.E.Leonowicz, A.S.Chu, S.B.McCullen, I.D.Johnson, E.W.Sheppard; *Chem.Mater.*, **6**, 2070-2077 (1994).
- [6] J.C.Vartuli, S.S.Shih, C.T.Kresge, J.S.Beck; *Stud.Surf.Sci.Catal.*, **117**, 13-21 (1998).
- [7] G.D.Stucky, A.Monnier, F.Schueth, Q.Huo, D.I.Margolese, D.Kumar, M.Krishnamurty, P.Petroff, A.Firouzi, M.Janicke, B.F.Chmelka; *Mol.Cryst.Liq.Cryst.*, **240**, 187-200 (1994).
- [8] Q.Huo, D.I.Margolese, G.D.Stucky; *Chem.Mater.*, **8** 1147-1160 (1996).
- [9] P.T.Tanev, M.Chibwe, T.J.Pinnavaia; *Nature*, **368**, 321-323 (1994).
- [10] E.Prouzet, T.J.Pinnavaia; *Angew.Chem.Int.Ed.*, **36**, 516-518 (1997).
- [11] T.J.Pinnavaia, W.Zhang; *Stud.Surf.Sci.Catal.*, **117**, 23-36 (1998).
- [12] F.Schuth, W.Schmidt; *Adv.Mater.*, **14**, 629-638 (2002).
- [13] G.Wirnsberger, P.Yang, B.J.Scott, B.F.Chmelka, G.D.Stucky; *Spectrochim.Acta A.*, **57**, 2049-2060 (2001).
- [14] W.Zhang, T.R.Pauly, T.J.Pinnavaia; *Chem.Mater.*, **9**, 2491-2498 (1997).
- [15] D.H.Li, Z.Chen, Y.Wan, X.J.Tu, Y.F.Shi, Z.X.Chen, W.Shen, C.Z.Yu, B.Tu, D.Y.Zhao; *J.Mater.Chem.*, **16**, 1511-1159 (2006).
- [16] J.M.Sun, H.Zhang, Ma, D.Y.Y.Chen, X.H.Bao, A.Klein-Hoffmann, N.Pfander, D.S.Su; *Chem. Commun.*, 5343-5345 (2005).
- [17] S.A.El-Safty, T.Hanaoka; *Chem.Mater.*, **16**, 384-400 (2004).
- [18] M.C.Burleigh, M.A.Markowitz, E.M.Wong, J.-S.Lin, B.P.Gaber; *Chem.Mater.*, **13**, 4411-4412 (2001).
- [19] Y.Liang, R.Anwander; *Micropor.Mesopor.Mater.*, **72**, 153-165 (2004).
- [20] Y.H.Yue, A.Gedeon, J.L.Bonardet, N.Melosh, J.B.D'Espinose, J.Fraissard; *Chem. Commun.*, 1967-1968 (1999).
- [21] P.T.Tanev, T.J.Pinnavaia; *Science*, **267**, 865-867 (1995).
- [22] A.Tuel; *Micropor.Mesopor.Mater.*, **27**, 151-169 (1999).
- [23] Y.Li, W.H.Zhang, L.Zhang, Q.H.Yang, Z.B.Wei, Z.C.Feng, C.Li; *J.Phys.Chem.B*, **108**, 9739-9744 (2004).
- [24] K.S.W.Sing, D.H.Everett, R.A.W.Haul, L.Moscou, R.A.Pierotti, J.Rouquerol, T.Siemieniewska; *Pure Appl.Chem.*, **57**, 603-619 (1985).
- [25] D.Y.Zhao, J.L.Feng, Q.S.Huo, N.Melosh, G.H.Fredrickson, B.F.Chmelka, G.D.Stucky; *Science*, **279**, 548-552 (1998).
- [26] D.Y.Zhao, Q.S.Huo, J.L.Feng, B.F.Chmelka, G.D.Stucky; *J.Am.Chem.Soc.*, **120**, 6024-6036 (1998).
- [27] F.D.Renzo; *J.Catal Today*, **41**, 37-40 (1998).
- [28] M.Busio, J.Janchen, J.H.C.Van Hooff; *Micropor. Mater.*, **5**, 211-218 (1995).